

Solving Heat Transfer Problem on a Stretching/Shrinking Surface with Convective Boundary Condition using *bvp4c* Solver

Noor Amalina Ehyak¹, Fazlina Aman^{1*}

¹ Department of Mathematics and Statistics, Faculty of Applied Sciences and Technology, UTHM Kampus Cawangan Pagoh, Hab Pendidikan Tinggi Pagoh, KM 1, Jalan Panchor, 86400 Pagoh, Muar, Johor, MALAYSIA.

*Corresponding Author: fazlina@uthm.edu.my

DOI: <https://doi.org/10.30880/ekst.2025.05.02.004>

Article Info

Received: 30 December 2024

Accepted: 18 January 2025

Available online: 19 December 2025

Keywords

Heat Transfer, Stretching/Shrinking, Convective Boundary Condition, Shooting Method, *bvp4c* Solver

Abstract

The heat transfer problem over a stretching/shrinking surface with a convective boundary condition is studied in this work. The objectives are to verify the governing equations, to generate a numerical solution and to analyse the problem. Using similarity transformations, the governing partial differential equations (PDEs) for heat transfer and fluid flow are converted into ordinary differential equations (ODEs). The MATLAB's *bvp4c* solver is used to obtain a numerical solution to the generated ODEs. An analysis is done on how the stretching/shrinking parameter, convective parameter, and Prandtl number affected the thermal boundary layer. The findings indicate that the local Nusselt number increases as the shrinking parameter increases. The opposite behaviour happens for the stretching parameter. As for the convective parameter, it reduced the thermal boundary layer thickness and enhanced heat transfer performance when it increased significantly. Besides, increasing the Prandtl number enhanced heat transfer for both stretching and shrinking cases. Additionally, the study compared the results with previous research to confirm the validity of the findings.

1. Introduction

Heat transfer over a stretching or shrinking surface is a critical field of study in fluid mechanics and thermal sciences because of its numerous commercial uses, such as polymer extrusion, glass fibre manufacture, and continuous sheet cooling. These processes often involve complex thermal interactions influenced by surface conditions, fluid properties, and heat transfer mechanisms, necessitating advanced mathematical modelling and computational techniques for accurate analysis and optimization.

Numerous studies have been conducted on the subject of heat transmission across a stretching or contracting surface while considering different physical properties such as magnetic fields, porosity, and slip velocity. Researchers such as [1] and [2] investigated the influence of thermal radiation, viscous dissipation, and magnetic fields on heat transfer in nanofluids and viscoelastic fluids. In order to get better understanding of solution stability and boundary layer behaviour, [3] and [4] investigated dual solutions for fluid flow and heat transfer over permeable and nonlinear stretching/shrinking surfaces.

Analysing boundary layer flows requires the use of convective boundary conditions, which define the heat exchange between a fluid and a surface. These conditions have been studied extensively in contexts involving nanofluids, thermal radiation, and viscous dissipation. [5] used the shooting method to solve the governing equations for his analysis of heat transport over a stretching/shrinking sheet under external uniform shear flow.

Their work, while foundational, revealed limitations such as convergence challenges and sensitivity to initial approximations when addressing complex boundary conditions or multiple solutions. Subsequent studies, including those by [6] and [7], expanded on these findings by investigating the impact of factors such as Brownian motion, Biot number, and Lorentz forces.

The development and application of numerical methods for boundary value problems (BVPs) have been pivotal in advancing the understanding of heat transfer phenomena. Techniques such as the Runge-Kutta Fehlberg algorithm, Chebyshev pseudospectral methods, and non-polynomial spline approaches have enabled the accurate solution of nonlinear ordinary differential equations derived from governing equations. [5] employed the shooting method to transform BVPs into initial value problems (IVPs), while [8] utilized the Chebyshev pseudospectral differentiation matrix for analytical and numerical solutions. Recent advancements, including the work of [9] and [10], have introduced innovative numerical methods to handle three-dimensional and eigenvalue problems, further enriching the field.

Among these numerical techniques, the `bvp4c` solver in MATLAB has emerged as a robust tool for solving BVPs. This finite difference-based solver, featuring adaptive mesh refinement and collocation methods, has been utilized in recent studies to address various heat transfer and flow problems, offering enhanced stability and computational efficiency. [11] and [12] applied `bvp4c` to solve nonlinear systems, revealing its effectiveness in capturing velocity, temperature, and concentration profiles. [13] and [14] demonstrated its ability to handle transformed ODEs from similarity transformations, yielding comprehensive graphical and numerical data.

Despite these advancements, there remains a need for comparative analyses to evaluate the effectiveness of numerical solvers in solving complex heat transfer problems under convective boundary conditions. In order to fill this gap, this work uses the `bvp4c` solver to examine the heat transfer properties as a boundary layer flows over a stretching/shrinking surface. Building on the work of [5], the present study aims to validate the conversion using similarity transformations to use the `bvp4c` solver to transform partial differential equations (PDEs) to ordinary differential equations (ODEs) and compare the numerical solutions with results from traditional shooting methods. By doing this, this study aims to analyse the benefits of current numerical techniques for solving BVPs in thermal sciences and offer better comprehension of the behaviour of heat transfer processes.

Nomenclature

k	Thermal conductivity of the fluid
L	Characteristic length of the sheet
q_w	Surface heat flux
T_f	Convective fluid temperature below the moving sheet
T_w	Surface temperature
T_∞	Ambient temperature
U_w	The reference stretching/shrinking velocity of the sheet

Greek Symbols

k	Thermal diffusivity
η	Similarity variable
θ	Dimensionless fluid temperature
μ	Dynamic viscosity
ν	Kinematic viscosity
ρ	Fluid density

Subscripts

f	Base fluid
h_f	Convective heat transfer coefficient

2. Research Methodology

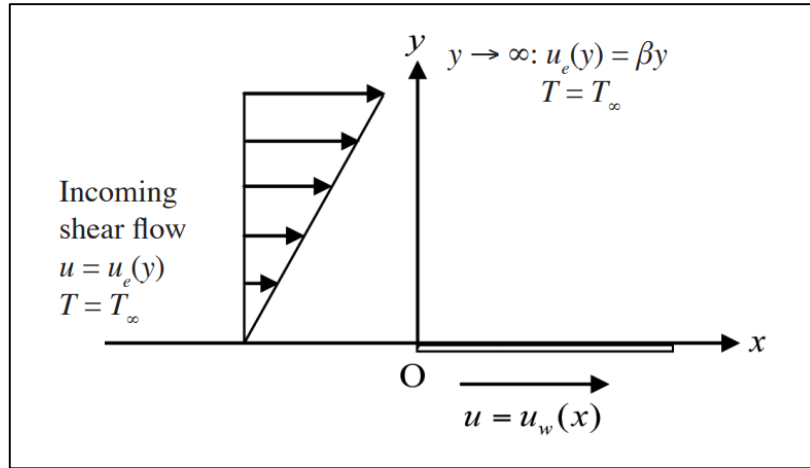


Fig. 1 Physical model and coordinate system [5]

Consider a two-dimensional steady boundary layer shear flow over a stretching/shrinking sheet at ambient temperature T_∞ as shown in Fig. 1. Assume the velocity of the stretching/shrinking sheet is $u_w(x) = U_w \left(\frac{x}{L}\right)^{\frac{1}{3}}$, while the velocity of the free stream is $u_e(y) = U_w \left(\frac{x}{L}\right)^{\frac{1}{3}}$, where x and y are Cartesian coordinates measured along the sheet and normal to it, respectively, L is the reference length, U_w is the reference stretching/shrinking velocity of the sheet, and β is the constant strain rate.

By referring to [5], the governing equation under the boundary layer approximations are:

$$\frac{\partial u}{\partial x} + \frac{\partial v}{\partial y} = 0, \tag{1}$$

$$u \frac{\partial u}{\partial x} + v \frac{\partial u}{\partial y} = \nu \frac{\partial^2 u}{\partial y^2}, \tag{2}$$

$$u \frac{\partial T}{\partial x} + v \frac{\partial T}{\partial y} = \alpha \frac{\partial^2 T}{\partial y^2}, \tag{3}$$

subject to the boundary conditions that can be expressed as:

$$v = 0, u = u_w(x) = U_w \left(\frac{x}{L}\right)^{\frac{1}{3}} \text{ at } y = 0. \tag{4}$$

$$u = u_e(y) = \beta y \text{ as } y \rightarrow \infty.$$

where u and v represent velocity components along the x and y axes respectively, T is the fluid temperature, α is the thermal diffusivity, and ν is the kinematic viscosity.

Following [5] the similarity transformation variables are as follows.

$$\psi = \nu \left(\frac{x}{L}\right)^{\frac{2}{3}} f(\eta), \theta(\eta) = \frac{T - T_\infty}{T_f - T_\infty}, \eta = \left(\frac{x}{L}\right)^{\frac{1}{3}} \frac{y}{L}, \tag{5}$$

where ψ is the stream function, with $u = \frac{\partial \psi}{\partial y}$ and $v = -\frac{\partial \psi}{\partial x}$.

By using similarity transformation variables [5], the equations (1) - (4) become

$$3f''' + 2ff'' - f'^2 = 0 \quad (6)$$

$$\frac{3}{Pr} \theta'' + 2f\theta' = 0 \quad (7)$$

where Pr is Prandtl number with corresponding boundary conditions as below

$$f(0) = 0, f'(0) = \lambda, \theta' = -\gamma[1 - \theta(0)] \quad (8)$$

$$f'(\eta) = \eta, \theta(\eta) \rightarrow 0 \text{ as } \eta \rightarrow \infty$$

The skin friction coefficient (C_f) and the local Nusselt number (Nu_x) are the physical quantity of interest in this study that can be written as follows [5]:

$$C_f = \frac{T_w}{\rho u_e^2} \text{ with } T_w = \mu \left(\frac{\partial u}{\partial y} \right)_{y=0} \quad (9)$$

$$Nu_x = \frac{xq_w}{k(T_f - T_\infty)} \text{ with } q_w = -k \left(\frac{\partial T}{\partial y} \right)_{y=0} \quad (10)$$

Substitute (9) and (10) to get equation (11) below,

$$\frac{1}{2} C_f Re_x = f''(0), Nu_x Re_x^{-\frac{1}{3}} = -\theta'(0) \quad (11)$$

where $Re_x^{\frac{1}{3}} = \left(\frac{\beta}{\nu} \right)^{\frac{2}{3}}$ is the local Reynold Number and μ is a dimensionless parameter, defined as $\mu = \rho\nu$.

3. Results and Discussion

The local Nusselt number, $-\theta'(0)$ for different stretching/shrinking parameters λ and Prandtl numbers (Pr) for the convective parameter $\gamma = 1$ is shown in Table 1. There are only slight variations in the comparison, which shows good agreement.

Table 1 indicates that the Nusselt number is rising as the stretching parameter λ rises for the stretching scenario ($\lambda > 0$). For example, the Nusselt number is 0.4315 [5] against 0.4254 (present results) at $\lambda=1$ and $Pr = 1$, and it increases to 0.5129 and 0.5062, respectively, at $\lambda=3$. The increased temperature is explained by a thinner thermal boundary layer caused by stronger strain, which improves heat transfer at the surface. Greater Nusselt numbers are also a result of greater Prandtl numbers. The Nusselt number for $Pr=1.7$ at $\lambda=1$, for instance, is 0.4897 [5] and 0.4842 (present results), highlighting the importance of fluid characteristics in improving heat transport.

The opposite pattern is observed in the shrinking case ($\lambda < 0$), where the Nusselt number falls as λ gets more negative. For example, the Nusselt numbers are 0.3372 [5] and 0.3392 (present data) for $\lambda = -0.1$ and $Pr = 1$, respectively, but they drastically decrease to 0.2077 and 0.2623 at $\lambda = -0.6$. The thickening of the thermal boundary layer in decreasing flows reduces the efficiency of heat transfer. However, Nusselt numbers are slightly higher than greater Prandtl numbers, just like in the stretching scenario.

Table 1 Values of the local Nusselt number $-\theta'(0)$ for different values of stretching/shrinking parameter λ and Prandtl number Pr when the convective parameter $\gamma = 1$

λ	Pr							
	0.72		1		1.5		1.7	
	[5]	Present results	[5]	Present results	[5]	Present results	[5]	Present results
Stretching case $-\theta'(0)$								
1	0.3971	0.3906	0.4315	0.4254	0.4757	0.4701	0.4897	0.4842
1.5	0.4206	0.4133	0.4577	0.4510	0.5048	0.4989	0.5196	0.5139
2	0.4401	0.4325	0.4791	0.4722	0.5282	0.5224	0.5435	0.5380
2.5	0.4568	0.4490	0.4972	0.4904	0.5477	0.5421	0.5633	0.5580
3	0.4714	0.4636	0.5129	0.5062	0.5644	0.5590	0.5802	0.5751
Shrinking case $-\theta'(0)$								
-0.1	0.3145	0.3165	0.3372	0.3392	0.3661	0.3681	0.3751	0.3772
-0.2	0.3021	0.3066	0.3227	0.3273	0.3486	0.3535	0.3566	0.3616
-0.3	0.2876	0.2957	0.3057	0.3142	0.3279	0.3371	0.3347	0.3441
-0.5	0.2466	0.2696	0.2571	0.2824	0.2680	0.2970	0.2706	0.3010
-0.6	0.2051	0.2533	0.2077	0.2623	0.2062	0.2712	0.2044	0.2732

Fig. 2 displays the temperature profiles $\theta(\eta)$ for a range of Prandtl numbers for $\lambda = 0.2$ and $\gamma = 1$. As the Prandtl number increases in both situations, the temperature profiles drop more quickly, suggesting that a thinner thermal boundary layer is caused by improved conduction in higher Pr fluids. Temperature profiles $\theta(\eta)$ for various stretching parameters of $\lambda (> 0)$ for Pr=1 and $\gamma = 1$ are displayed in Fig. 3. The temperature decreases more quickly along the η -axis as λ increases, as shown in the figure. This suggests a thinner thermal barrier layer and better heat transfer.

The temperature profiles $\theta(\eta)$ for different values of the shrinking parameter $\lambda (< 0)$ with Pr=1 and $\gamma = 1$ are shown in Fig. 4. The figure demonstrates that the temperature profiles decay more slowly as λ drops from -0.1 to -0.6, indicating less heat movement close to the surface and a stronger thermal barrier layer. The shrinking effect, which lowers the convection strength and raises thermal resistance, is responsible for the slower temperature decrease.

The temperature profiles $\theta(\eta)$ for different values of the convective parameter γ when, Pr=1, and $\lambda = 1$ are shown in Fig. 5. The temperature profiles exhibit a faster decrease along the η -axis as γ rises from 0.1 to 100. This behaviour implies that a higher convective parameter improves heat transfer while decreasing the thickness of the thermal boundary layer. In particular, the temperature distribution is more gradual for smaller values of γ , indicating weaker convection close to the surface. However, the temperature lowers dramatically if γ increases significantly, suggesting longer convective heat transfer effects.

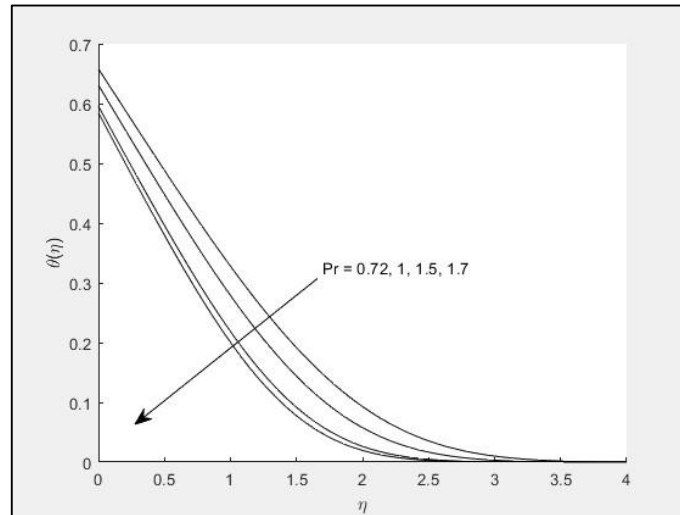


Fig. 2 Temperature profiles $\theta(\eta)$ for some values of Pr when $\lambda = 0.2$ and $\gamma = 1$

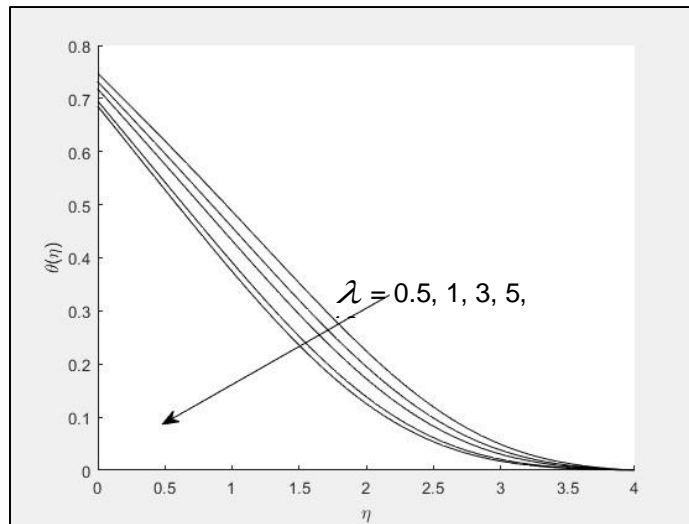


Fig. 3 Temperature profiles $\theta(\eta)$ for some values of $\lambda(> 0)$ when $Pr = 0.7$ and $\gamma = 1$

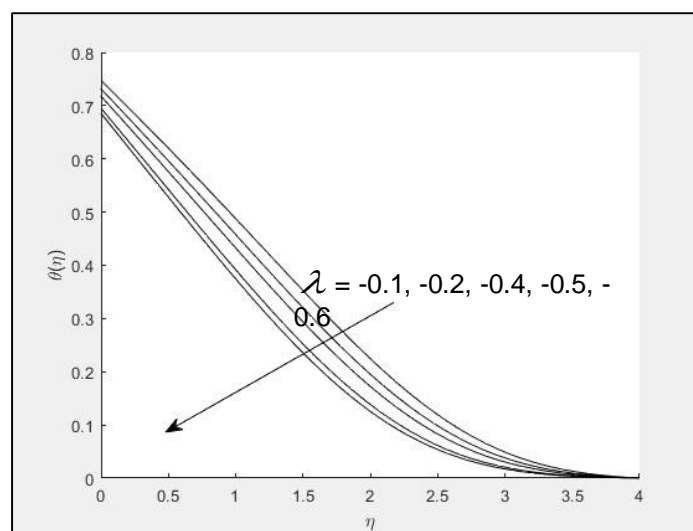


Fig. 4 Temperature profiles $\theta(\eta)$ for some values of $\lambda(< 0)$ when $Pr = 0.7$ and $\gamma = 1$

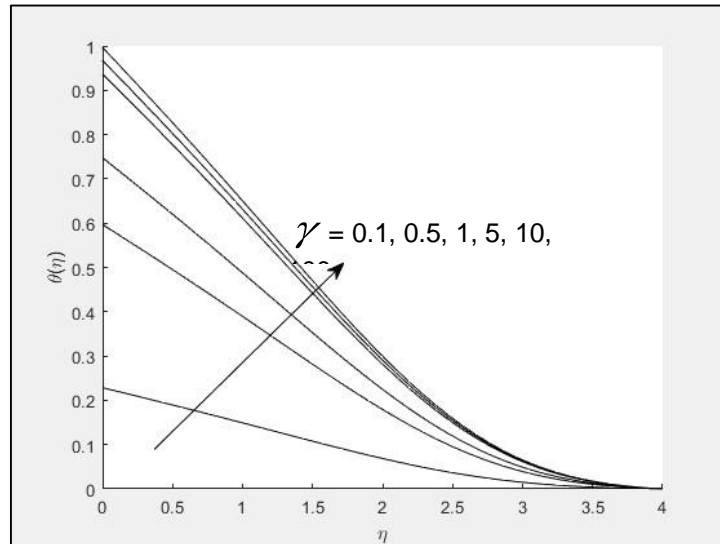


Fig. 5 Temperature profiles $\theta(\eta)$ for some values of γ when $Pr = 0.7$ and $\lambda = 1$

4. Conclusion

Heat transfer over a stretching/shrinking surface with a convective boundary condition has been successfully investigated in this work and achieved its objectives. The first objective is to use similarity transformations to verify the conversion from partial differential equations to ordinary differential equations has been accomplished. Second, the numerical solution has been generated by using shooting method with bvp4c solver in MATLAB software. Third, a comparison and analysing the effect on temperature profile with various parameters such as stretching/shrinking parameters, Prandtl number, and the convective parameter has been discussed as follows:

- As for the stretching case ($\lambda > 0$), the results demonstrated that the local Nusselt number increases as λ increases.
- Different with the shrinking case ($\lambda < 0$), the results demonstrated that the local Nusselt number decreased as λ decrease.
- An increase in the Prandtl number enhanced heat transfer for both stretching and shrinking cases.
- Increasing the convective parameter, γ significantly reduced the thermal boundary layer thickness and enhanced heat transfer performance.

Then, the results of this study are compared with those of [5] to validate the findings, showing a strong agreement between the two.

Acknowledgement

The authors would like to thank the Faculty of Applied Sciences and Technology, Universiti Tun Hussein Onn Malaysia for its support.

Conflict of Interest

Authors declare that there is no conflict of interest regarding the publication of the paper.

Author Contribution

The authors confirm contribution to the paper as follows: **study conception and design:** Noor Amalina Ehyak; **solve the governing equations:** Noor Amalina Ehyak; **analysis and interpretation of results:** Noor Amalina Ehyak, Fazlina Aman; **draft manuscript preparation:** Noor Amalina Ehyak, Fazlina Aman. All authors reviewed the results and approved the final version of the manuscript.

References

- [1] M. Turkyilmazoglu, "Three dimensional MHD flow and heat transfer over a stretching/shrinking surface in a viscoelastic fluid with various physical effects," *Int J Heat Mass Transf*, vol. 78, pp. 150–155, 2014, doi: 10.1016/j.ijheatmasstransfer.2014.06.052.

- [2] D. Pal, G. Mandal, and K. Vajravelu, "Flow and heat transfer of nanofluids at a stagnation point flow over a stretching/shrinking surface in a porous medium with thermal radiation," *Appl Math Comput*, vol. 238, pp. 208–224, Jul. 2014, doi: 10.1016/j.amc.2014.03.145.
- [3] R. Jusoh, R. Nazar, and I. Pop, "Flow and heat transfer of magnetohydrodynamic three-dimensional Maxwell nanofluid over a permeable stretching/shrinking surface with convective boundary conditions," *Int J Mech Sci*, vol. 124–125, pp. 166–173, May 2017, doi: 10.1016/j.ijmecsci.2017.02.022.
- [4] A. Jaafar, I. Waini, A. Jamaludin, R. Nazar, and I. Pop, "MHD flow and heat transfer of a hybrid nanofluid past a nonlinear surface stretching/shrinking with effects of thermal radiation and suction," *Chinese Journal of Physics*, vol. 79, pp. 13–27, Oct. 2022, doi: 10.1016/j.cjph.2022.06.026.
- [5] F. Aman, A. Ishak, and I. Pop, "Heat Transfer at a Stretching/Shrinking Surface Beneath an External Uniform Shear Flow with a Convective Boundary Condition," *Sains Malaysiana* 40(12), pp. 1369–1374, 2011.
- [6] N. A. Othman, N. A. Yacob, N. Bachok, A. Ishak, and I. Pop, "Mixed convection boundary-layer stagnation point flow past a vertical stretching/shrinking surface in a nanofluid," *Appl Therm Eng*, vol. 115, pp. 1412–1417, 2017, doi: 10.1016/j.applthermaleng.2016.10.159.
- [7] M. Hussain *et al.*, "MHD thermal boundary layer flow of a Casson fluid over a penetrable stretching wedge in the existence of nonlinear radiation and convective boundary condition," *Alexandria Engineering Journal*, vol. 60, no. 6, pp. 5473–5483, Dec. 2021, doi: 10.1016/j.aej.2021.03.042.
- [8] E. H. Aly and K. Vajravelu, "Exact and numerical solutions of MHD nano boundary-layer flows over stretching surfaces in a porous medium," *Appl Math Comput*, vol. 232, pp. 191–204, Apr. 2014, doi: 10.1016/j.amc.2013.12.147.
- [9] W. H. Mitchell, H. G. Bell, Y. Mori, L. Ohm, and D. Spirn, "A single-layer based numerical method for the slender body boundary value problem," *J Comput Phys*, vol. 450, Feb. 2022, doi: 10.1016/j.jcp.2021.110865.
- [10] R. B. Kudenatti, N. E. Misbah, and M. C. Bharathi, "A numerical study on boundary layer flow of Carreau fluid and forced convection heat transfer with viscous dissipation and generalized thermal conductivity," *Math Comput Simul*, vol. 208, pp. 619–636, Jun. 2023, doi: 10.1016/j.matcom.2023.01.026.
- [11] A. Tanveer, T. Salahuddin, M. Khan, A. S. Alshomrani, and M. Y. Malik, "The assessment of nanofluid in a Von Karman flow with temperature relied viscosity," *Results Phys*, vol. 9, pp. 916–922, Jun. 2018, doi: 10.1016/j.rinp.2018.03.051.
- [12] S. Zaman and M. Gul, "Magnetohydrodynamic bioconvective flow of Williamson nanofluid containing gyrotactic microorganisms subjected to thermal radiation and Newtonian conditions," *J Theor Biol*, vol. 479, pp. 22–28, Oct. 2019, doi: 10.1016/j.jtbi.2019.02.015.
- [13] U. Farooq, M. A. Ijaz, M. I. Khan, S. S. P. M. Isa, and D. C. Lu, "Modeling and non-similar analysis for Darcy-Forchheimer-Brinkman model of Casson fluid in a porous media," *International Communications in Heat and Mass Transfer*, vol. 119, Dec. 2020, doi: 10.1016/j.icheatmasstransfer.2020.104955.
- [14] N. Amar and N. Kishan, "The influence of radiation on MHD boundary layer flow past a nano fluid wedge embedded in porous media," *Partial Differential Equations in Applied Mathematics*, vol. 4, Dec. 2021, doi: 10.1016/j.padiff.2021.100082.